

RESEARCH ARTICLE

Reduced gray matter volume and cortical thickness associated with traffic-related air pollution in a longitudinally studied pediatric cohort

Travis Beckwith^{1,2}*, Kim Cecil², Mekibib Altaye³, Rachel Severs⁴, Christopher Wolfe³, Zana Percy⁵, Thomas Maloney², Kimberly Yolton⁶, Grace LeMasters⁵, Kelly Brunst⁵, Patrick Ryan³



1 Molecular Epidemiology in Children's Environmental Health Training Program, Department of Environmental Health, University of Cincinnati College of Medicine, Cincinnati, Ohio, United States of America, **2** Imaging Research Center, Department of Radiology, Cincinnati Children's Hospital Medical Center and the University of Cincinnati College of Medicine, Cincinnati, Ohio, United States of America, **3** Division of Biostatistics and Epidemiology, Department of Pediatrics, Cincinnati Children's Hospital Medical Center and the University of Cincinnati College of Medicine, Cincinnati, Ohio, United States of America, **4** Department of Psychology, Western Kentucky University, Bowling Green, Kentucky, United States of America, **5** Department of Environmental Health, University of Cincinnati College of Medicine, Cincinnati, Ohio, United States of America, **6** Division of General and Community Pediatrics, Department of Pediatrics, Cincinnati Children's Hospital Medical Center and the University of Cincinnati College of Medicine, Cincinnati, Ohio, United States of America

* These authors contributed equally to this work.

* Travis.Beckwith@cchmc.org

OPEN ACCESS

Citation: Beckwith T, Cecil K, Altaye M, Severs R, Wolfe C, Percy Z, et al. (2020) Reduced gray matter volume and cortical thickness associated with traffic-related air pollution in a longitudinally studied pediatric cohort. PLoS ONE 15(1): e0228092. <https://doi.org/10.1371/journal.pone.0228092>

Editor: Emanuele Bartolini, Nuovo Ospedale Prato (NOP) Santo Stefano, USL Toscana Centro, ITALY

Received: October 2, 2019

Accepted: January 7, 2020

Published: January 24, 2020

Copyright: © 2020 Beckwith et al. This is an open access article distributed under the terms of the [Creative Commons Attribution License](https://creativecommons.org/licenses/by/4.0/), which permits unrestricted use, distribution, and reproduction in any medium, provided the original author and source are credited.

Data Availability Statement: The data and code used in the study are not available in the public domain. Data usage is currently governed by the Institutional Review Board at Cincinnati Children's Hospital Medical Center. The data contains sensitive information and is confidential. De-identified data will be provided following CCHMC IRB approval. Please contact the corresponding author for data requests. The CCHMC IRB may be reached via email at irb@cchmc.org or ORCRA@cchmc.org, or by phone at 513.636.8039.

Abstract

Early life exposure to air pollution poses a significant risk to brain development from direct exposure to toxicants or via indirect mechanisms involving the circulatory, pulmonary or gastrointestinal systems. In children, exposure to traffic related air pollution has been associated with adverse effects on cognitive, behavioral and psychomotor development. We aimed to determine whether childhood exposure to traffic related air pollution is associated with regional differences in brain volume and cortical thickness among children enrolled in a longitudinal cohort study of traffic related air pollution and child health. We used magnetic resonance imaging to obtain anatomical brain images from a nested subset of 12 year old participants characterized with either high or low levels of traffic related air pollution exposure during their first year of life. We employed voxel-based morphometry to examine group differences in regional brain volume, and with separate analyses, changes in cortical thickness. Smaller regional gray matter volumes were determined in the left pre- and post-central gyri, the cerebellum, and inferior parietal lobe of participants in the high traffic related air pollution exposure group relative to participants with low exposure. Reduced cortical thickness was observed in participants with high exposure relative to those with low exposure, primarily in sensorimotor regions of the brain including the pre- and post-central gyri and the paracentral lobule, but also within the frontal and limbic regions. These results suggest that significant childhood exposure to traffic related air pollution is associated with structural alterations in brain.

Funding: This work was funded by the National Institute for Environmental Health Sciences (NIEHS; <https://www.niehs.nih.gov/>), award numbers R01 ES019890 (P.R.), R01 ES027224 (K. Y.), and R01 ES026446 (K.C.); the National Center for Advancing Translational Sciences of the National Institutes of Health (NCATS; <https://ncats.nih.gov/>), award number UL1 TR001425; and a National Institutes of Health (NIH; <https://www.nih.gov/>; <https://researchtraining.nih.gov/programs/training-grants/T32>) training grant awarded to the Molecular Epidemiology in Children's Environmental Health Training Program (MECEH), award number T32-ES10957. The funders had no role in study design, data collection and analysis, decision to publish, or preparation of the manuscript.

Competing interests: The authors have declared that no competing interests exist.

Introduction

Accumulating evidence suggests traffic-related air pollution (TRAP) is a contributor to both neurodegenerative diseases and neurodevelopmental disorders [1–9]. TRAP consists of a complex mixture of gaseous pollutants, fine and ultrafine particulate matter, heavy metals, elemental and organic carbon, polycyclic aromatic hydrocarbons, and other dynamic constituents [10]. Diesel exhaust (DE) is a significant contributor to TRAP with a composition incorporating ultrafine particulate matter (UFP; <100 nm) and more than 40 toxic pollutants [4, 10]. UFP can readily access the brain directly through the nasal olfactory mucosa via the olfactory bulb; this direct entry sets up a scenario for adverse structural consequences to occur in the brain due to the presence of TRAP despite a potentially low translocation rate from deposition in the nasal cavity [11–13].

Advancements in computational image analysis methods [14–16] reveal typical brain development as well as advance discovery of pathophysiological mechanisms associated with aberrant development and injury, including those from environmental exposures. Structural magnetic resonance imaging (MRI) derived cortical thickness assessment estimates the distance from the pial surface to the gray/white interface surface via automated reconstruction methods. Cortical thickness measures reflect the size, density and arrangement of neurons, neuroglia and nerve fibers while also reflecting axon and dendrite remodeling, and myelination as myelin proliferation into the cortical neuropil replaces gray matter during development [17–21]. The measurement of cortical thickness [17, 22] pairs well with other whole brain MRI analysis techniques such as voxel based morphometry (VBM) which determines brain volume based on tissue class via a voxel-wise comparison of anatomical images [17–21]. VBM allows for detection of regional and global differences in volume including decreases or increases in gray and/or white matter [23–25]. For gray matter, VBM includes cortical surface area and cortical thickness. These complimentary methods characterize brain structure [25].

By comparing adolescents exposed to high and low concentrations of TRAP during the first year of life, we ascertained if there was evidence that early life exposure to TRAP was associated with changes in brain structure, specifically brain volume and cortical thickness. We hypothesized that participants with the highest early life TRAP exposures would demonstrate atypical neural development with reduced regional brain volumes and cortical thickness at age 12 years compared to those with lowest TRAP exposures. If early life TRAP exposure irreversibly harms brain development, as with infection or teratogen exposure, structural consequences could persist regardless of the time point for a subsequent examination. However, the study was exploratory as identification of regions with alterations in brain volume and cortical thickness informs potential mechanisms and provides functional significance on how pollutants exert their effects in the brain.

Materials and methods

Study enrollment

Participants in this study are a subset of the previously described Cincinnati Childhood Allergy and Air Pollution Study (CCAAPS) cohort [26, 27]. Briefly, CCAAPS is a prospective cohort study of children recruited prior to age 6 months to examine early childhood exposure to TRAP and health outcomes including allergic diseases, asthma, and neurodevelopment. Eligibility for study enrollment included participants born at a gestational age greater than 35 weeks, a birth record address either < 400 meters (m) or > 1500 m from a major highway, and at least one biological parent with an allergic disease. Participating children and their caregivers completed clinical visits at ages 1, 2, 3, 4, 7, and 12 years (y). Caregivers completed study

questionnaires at each study visit regarding their child's health and general wellbeing, housing characteristics, and residential history. At all study visits children completed allergy testing and physical examinations, including assessment for growth, anthropometry, and developmental milestones. The clinic visit at age 12 y included direct and indirect assessments of intelligence, reading ability, executive function, mental health, and other neurodevelopmental outcomes. A nested imaging substudy was conducted on subset of CCAAPS participants at the age 12 y study visit with eligibility details described below. The Institutional Review Boards at the University of Cincinnati and the Cincinnati Children's Hospital Medical Center (CCHMC) approved the study protocol. Participants provided written assent prior to participation. Participant's parents and legal guardians provided informed consent prior to participation.

Exposure to traffic-related air pollution

Childhood exposure to TRAP was estimated for study participants using a previously developed and validated land-use regression (LUR) model [28, 29]. Briefly, an ambient air sampling network consisting of 27 sampling sites was operated from 2001–2006 in the greater Cincinnati area, and 24-hour sampling was conducted simultaneously at 4–5 sites over different seasons [29]. Particulate matter less than 2.5 micrometers ($PM_{2.5}$) samples were collected on 37-mm Teflon membrane filters and 37-mm quartz filters with Harvard-type Impactors. $PM_{2.5}$ mass concentrations were determined by gravimetric analysis [30]. Teflon filters were analyzed by X-ray fluorescence to determine the elemental concentration of 39 elements and quartz filters were analyzed by thermal-optical transmittance using the NIOSH-5040 method to determine elemental and organic carbon concentrations. A multivariate receptor model, UNMIX, was used to identify significant sources contributing to $PM_{2.5}$ concentrations, including traffic. In order to estimate the specific fraction of the sampled elemental carbon arising from diesel exhaust, we applied elemental source profiles obtained from measurements conducted at cluster sources of diesel-fueled trucks and buses [30]. Thus, the fraction of the sampled elemental carbon due to diesel combustion was derived from each sampling day and is referred to as the elemental carbon attributable to traffic (ECAT), [30, 31]. Daily ECAT concentrations averaged over the entire monitoring period at the sampling sites ranged from 0.22–1.02 $\mu\text{g}/\text{m}^3$ and served as the dependent variable in our LUR model development [29]. LUR predictor variables included elevation, nearby truck traffic, and bus routes [29]. The final LUR model was applied to all residential locations of CCAAPS participants beginning at the birth record address and through age 12 y as reported by caregivers to derive time-weighted estimates of ECAT exposure throughout childhood [28, 29].

Nested imaging substudy eligibility

High-resolution anatomical imaging was acquired on a subset of CCAAPS participants who completed the age 12 y study visit. The intent of the nested imaging substudy was to identify differential imaging outcomes in children exposed to high levels of TRAP during early childhood compared to children exposed to low TRAP levels. Therefore, eligible participants whose estimated ECAT exposure from birth through age one year were in the highest or lowest quartiles of exposure, or whose birth record address was less than 400 m from a major road were recruited to participate in the nested imaging substudy. These participants were contacted about completing the imaging when scheduling the 12 y clinic visit, screened for exclusions or contraindications to MRI, such as non-removable dental appliances, braces, implanted devices, or known to be claustrophobic, and enrolled in the nested imaging substudy.

Participant characteristics

A total of 147 children were enrolled in the nested imaging substudy. Of these, imaging data was not available for 12 participants due to issues with image reconstruction, artifacts or incidental structural brain abnormalities that interfere with image processing. Demographic and other characteristics of the 135 participants included in this analysis are presented in Table 1. Overall, participants in the substudy were 56.3% male, 74.8% Caucasian, and were similar to participants who completed the age 12 clinic visit and the overall CCAAPS cohort with respect to demographic characteristics (Table 1). The majority were singleton births (127 (94%)) and right handed (126 (93%)). Table 2 presents the distribution of participant characteristics by early childhood TRAP exposure status. As expected from the design, the mean estimated ECAT exposure at the birth record address was twice as high in the high exposed group compared to the low exposed group (0.56 [0.13] versus 0.27 [0.02] $\mu\text{g}/\text{m}^3$, respectively). In addition, a greater proportion of participants in the substudy with high ECAT exposure were more likely to be African-american with reported annual household incomes < \$20,000 at initial study enrollment (Table 1).

Image acquisition

The participant MRI examinations were acquired using a 3T Achieva scanner (Philips Medical Systems, Best, Netherlands) equipped with a 32-channel head coil. High-resolution, three

Table 1. Characteristics of CCAAPS participants at enrollment, age 12 y, and imaging subset [n(%) or mean (SD)].

Characteristic (unit)	Enrollment n = 762	Age 12 y n = 344	MRI n = 135
<i>Child characteristics</i>			
Sex			
Male	415 (54.5%)	191 (55.5%)	76 (56.3%)
Female	347 (45.5%)	153 (44.5%)	59 (43.7%)
Race / Ethnicity			
Caucasian	587 (77.0%) (77.4%)	261 (75.9%)	101 (74.8%)
African American / More than one race	175 (23.0%) (22.6%)	83 (24.1%)	34 (25.2%)
Birth weight (lbs)	7.5 (1.2)	7.6 (1.2)	7.6 (1.2)
Duration of breastfeeding (months)	5.7 (6.5)	6.3 (6.9)	5.6 (6.9)
<i>Maternal characteristics</i>			
Age at study enrollment (years)	30.0 (5.7)	30.7 (5.9)	29.7 (5.7)
Maternal education at child age 1			
≤ High school	185 (24.9%)	72 (21.6%)	36 (27.7%)
Some college or trade school	196 (26.4%)	94 (28.1%)	31 (23.9%)
≥ College degree	361 (48.7%)	168 (50.3%)	63 (48.5%)
<i>Household characteristics</i>			
Household income (Parental report at first study visit)*			
< \$20,000	129 (17.5%)	58 (17.5%)	28 (21.5%)
\$20,000 to < \$40,000	129 (17.5%)	54 (16.3%)	22 (16.9%)
\$40,000 to < \$90,000	210 (28.5%)	95 (28.6%)	33 (25.4%)
\$90,000 to < \$110,000	196 (26.6%)	89 (26.8%)	36 (27.7%)
> \$110,000	73 (9.9%)	36 (10.8%)	11 (8.5%)
ECAT at birth record address ($\mu\text{g} / \text{m}^3$)	0.39 (0.13)	0.39 (0.14)	0.44 (0.18)

*Missing values (~3%) were not reported by parents

<https://doi.org/10.1371/journal.pone.0228092.t001>

Table 2. Model variables evaluated in the nested imaging substudy cohort.

Characteristic	Cohort (N = 135)	Range	Low exposure (N = 59)	High exposure (N = 76)	F or χ^2	P-value
Race: African American ¹	34 (~25%)		6 (~10%)	28 (~37%)	12.54	0.0004
Sex ¹	59 Female (~44%)		29 Female (~49%)	30 Female (~39.5%)	1.26	0.2608
ECAT at birth record address ²	0.44 (± 0.17)	0.24–0.88	0.27 (± 0.02)	0.56 (± 0.13)	286.06	< 0.0001
ECAT at imaging ²	0.38 (± 0.13)	0.24–0.83	0.30 (± 0.06)	0.44 (± 0.14)	54.20	< 0.0001
Average ECAT ²	0.39 (± 0.13)	0.24–0.85	0.29 (± 0.03)	0.48 (0.11)	163.33	< 0.0001
Child birth weight (pounds) ²	7.62 (± 1.26)	4.44–10.90	7.86 (± 1.31)	7.42 (± 1.19)	4.20	0.0423
Child age at imaging (years) ²	12.12 (± 0.75)	11.0–14.71	12.23 (± 0.80)	12.03 (± 0.7)	2.43	0.1211
Maternal age (years) ²	29.7 (± 5.7)	18.34–43.1	31.95 (± 5.01)	27.96 (± 5.62)	18.44	< 0.0001
Child FSIQ ²	99.32 (± 15.9)	44–139	101.9 (± 15.33)	97.3 (± 16.13)	3.91	0.097
Maternal IQ ²	105.11 (± 13.28)	65–145	109.24 (± 12.02)	101.91 (± 13.39)	10.87	0.0013
Deprivation index at birth ²	0.45 (± 0.19)	0.18–1.0	0.36 (± 0.1)	0.53 (± 0.21)	29.80	< 0.0001

Data presented as mean (\pm S.D.) or n (%)

F, χ^2 , and P-values represent comparison between low and high exposure groups

¹ Chi-square test

² One-way ANOVA

<https://doi.org/10.1371/journal.pone.0228092.t002>

dimensional, anatomical imaging data were collected using a single-shot turbo field echo (TFE) pulse sequence operating with an 8.2 milliseconds (ms) repetition time, a 3.7 ms echo time, a 1057 ms inversion time, a 8° flip angle, a sensitivity encoding (SENSE) factor of 2 (right-left) and 1 mm³ resolution.

Image processing

Anatomical images were reconstructed using Cincinnati Children's Image Processing Software (<https://irc.cchmc.org/software/cchips.php>) running in IDL 8.1 (Exelis Visual Information Solutions, Boulder CO). Images were then imported into Statistical Parametric Mapping 12 (SPM12) version 6685 (Wellcome Department of Cognitive Neurology, London) running in Matlab 7.13.0.564 (The Mathworks, Inc., Natick, MA). All images were first visually scanned for artifacts and any other abnormalities. Images were then manually reoriented so that the anterior and posterior commissures were in the same axial slice with the origin voxel [0, 0, 0] set medially on the anterior commissure. This step ensures that all images are in the same general orientation prior to processing and reduces the number of errors encountered during processing. Reoriented images were then processed using the Computational Anatomy Toolbox (CAT) version r1113 (<http://www.neuro.uni-jena.de/cat/>) for SPM12 [32]. A more detailed description of the initial image processing can be found in the methods of Beckwith, Dietrich [33]. Please see S1 Fig. for a simplified visual of the CAT12 workflow. Briefly, images were skull stripped, reoriented to a template in Montreal Neurological Institute (MNI) space using affine registration, segmented into tissue classes, and processed to minimize noise and partial volume effects [34]. The diffeomorphic anatomical registration through exponentiated line algebra (DARTEL) toolbox [35] within SPM12 was then used to apply a nonlinear deformation to the images utilizing an IXI-database template (<http://www.brain-development.org>). Normalized images were then bias-corrected and modulated by scaling the Jacobian determinants to account for differences in the tissue volume that occur during normalization. Normalized gray and white matter tissue probability maps were smoothed using an 8 mm Gaussian kernel.

The calculation of cortical thickness is included as an optional step in the VBM segmentation pipeline for the CAT toolbox. A projection based thickness [36] technique estimates the

white matter distance during the segmentation procedure and projects the local maxima onto neighboring gray matter voxels using the relationship to that distance. This distance is representative of cortical thickness. This technique permits the use of partial volume data, as well as sulcal asymmetries and blurring without requiring sulcal reconstruction [37]. To account for topological variations, a technique utilizing spherical harmonics was incorporated [38]. Spherical mapping [39] was used to permit the use of a shared coordinate system, and an adaptation of the DARTEL algorithm [35] was used for surface registration [40]. Cortical thickness images were then smoothed to 15 mm as recommended in the CAT12 manual.

Statistical analyses

Demographic characteristics, imputations of missing demographic variables, collinear relationships and covariate selection for the models were carried out in SAS software (SAS Institute, Cary, NC). Comparisons between participant characteristics were made using a Chi-Square test for categorical variables, and a one-way analysis of variance (ANOVA) for all other variables. Missing data points were generated using a multivariate normal distribution multiple imputation model in SAS. The rate of missing variables was not predicted by any variables in the imputation analysis and data points were assumed to be missing at random. Ten data sets were imputed using the PROC MI procedure. Parameter estimates for each imputed data set were generated via a general linear model and a pooled analysis was conducted to estimate the standard error for the imputed data set and compared to the initial estimate.

To account for the spatial features within the imaging analyses, we also employed SPM12 running in Matlab for the statistical analyses relating to imaging derived cortical thickness and VBM. Within SPM12, a full-factorial model allowed for differences in cortical thickness, gray matter volume, and white matter volume between the two exposure groups. Participants were grouped by exposure status (low ECAT, high ECAT) and sex. Main effects for exposure status and sex were initially explored using an omnibus F-test. An F-test was also used to explore the possibility of an interaction between exposure status and sex. In the event of a statistically significant finding, post-hoc T-tests were used to establish the directionality of the effect. Threshold-Free Cluster Enhancement (TFCE) [41, 42] was utilized for cluster-based statistics. Thresholds for the analyses were set using a Family-Wise Error (FWE) corrected P-value of 0.05 to correct for multiple comparisons.

Covariate selection

Variables considered for inclusion as covariates were: age at time of MRI examination, handedness, gestational age, birth weight, maternal IQ ascertained using the Wechsler Abbreviated Scale of Intelligence—2nd Edition, participant full scale IQ obtained using the Wechsler Intelligence Scale for Children—Fourth Edition (WISC-IV), race, sex and a previously calculated index measure of census tract deprivation index at birth [43]. Variables at the census-tract level contributing to the deprivation index include the median household income, fraction of households with income below the poverty level, educational attainment, health insurance coverage, households receiving public assistance and vacant houses. Sex was included as a factor in the analyses. Age at MRI examination [44], birth weight [45, 46], participant full scale IQ [47], census tract deprivation status at birth [43], and race [48, 49] were selected for inclusion in the final model. Total intracranial volume was also included as a covariate for volumetric analyses. Furthermore, because aspects of socioeconomic status were incorporated into the census tract deprivation index metric, variables such as income and educational attainment were not included as separate covariates in the final analyses.

Data and code availability statement

The data and code used in the study are not available in the public domain. Data usage is currently governed by the Institutional Review Board at Cincinnati Children's Hospital Medical Center. The data contains sensitive information and is confidential. The investigators will share de-identified data following approved institutional review board (IRB) policies. Investigators may request de-identified data by contacting the corresponding author. The CCHMC IRB can be reached at irb@cchmc.org, ORCRA@cchmc.org, or by phone at 513.636.8039.

Results

Upon direct comparison, we found decreased cortical thickness in the high ECAT group relative to the low ECAT group before and after adjusting for covariates. The reduction in cortical thickness for the somatosensory region was approximately 3% upon comparing the average values for high ECAT group relative to the low ECAT group. In the left hemisphere, regions of reduced cortical thickness were observed in the paracentral lobule, pre- and post-central gyri, precuneus, superior frontal gyrus, and superior parietal lobule (Fig 1, Table 3). In the right hemisphere, reduced cortical thickness was observed in the postcentral gyrus, paracentral lobule, posterior cingulate, superior frontal gyrus, and superior parietal lobule (Fig 1, Table 3). No main effects for sex were observed, nor was an interaction between ECAT exposure and sex present.

Volumetric analyses revealed reduced gray matter in the high versus low ECAT group before and after adjusting for covariates. Volumetric differences were observed in two regional clusters. The first cluster was located bilaterally in the cerebellum and extended to the right parietal cortex (Fig 2, Table 4). The second cluster was located primarily in the parietal lobe, including the pre- and post-central gyri, inferior parietal lobule, and supramarginal gyrus (Fig 2, Table 4). The volumetric reduction was approximately 4% upon comparing the average values for high versus low ECAT group. A small main effect for sex was also observed, with females displaying reduced gray matter volumes in frontal sub-lobar regions (not shown). However, no interaction between ECAT group and sex was detected. Furthermore, no volumetric differences were seen in any of the white matter analyses.

Discussion

Overall findings

Our study found a bilateral, medial region of reduced cortical thickness within the posterior frontal and anterior parietal lobes with early life high exposure to TRAP. Within the posterior

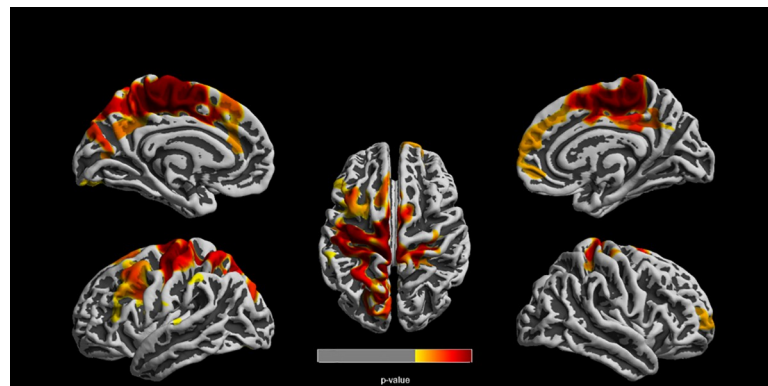


Fig 1. Statistically significant clusters using threshold free cluster enhancement. Clusters represent reduced cortical thickness in the high ECAT group compared to the low ECAT group. Clusters were corrected for multiple comparisons using a familywise error rate of $p \leq 0.05$.

<https://doi.org/10.1371/journal.pone.0228092.g001>

Table 3. Reduced cortical thickness in high ECAT exposure group compared to low ECAT exposure group with covariates.

Anatomical region	Cluster size (vertices)	Peak vertex MNI coordinates (X, Y, Z)	Vertex p-value
<u>Left hemisphere</u>			
Anterior cingulate Medial frontal gyrus Paracentral lobule Postcentral gyrus Precentral gyrus Precuneus Superior frontal gyrus Superior parietal lobule	31070	-16-43 56 -8-39 55 -4-17 59	0.006 0.006 0.006
Middle frontal gyrus Precentral gyrus	5350	-44 16 47 -34 10 29 -41 12 39	0.022 0.022 0.022
Fusiform gyrus	604	-21-92-12 -37-80-16	0.044 0.048
Inferior parietal lobule	279	8-33 4	0.049
<u>Right hemisphere</u>			
Cingulate Medial frontal gyrus Paracentral lobule Postcentral gyrus Superior frontal gyrus Ventromedial prefrontal cortex	16292	5-18 56 6-27 59 4-35 55	0.007 0.007 0.009
Postcentral gyrus	191	44-19 38	0.049

Vertices and clusters corrected for multiple comparisons (FWE) at $P < 0.05$ using TFCE; ECAT = Elemental carbon attributable to traffic; FWE = Familywise error rate; MNI = Montreal neurological institute; TFCE = Threshold free cluster enhancement

<https://doi.org/10.1371/journal.pone.0228092.t003>

frontal lobe, the precentral gyrus serves as the primary motor cortex and is responsible for executing voluntary movements through connections to the spinothalamic tract [50]. Immediately posterior, the parietal lobe with the postcentral gyrus is the primary sensory area. It is a topographically organized, functionally defined area responsible for integrating somatosensory information such as touch and proprioception [51].

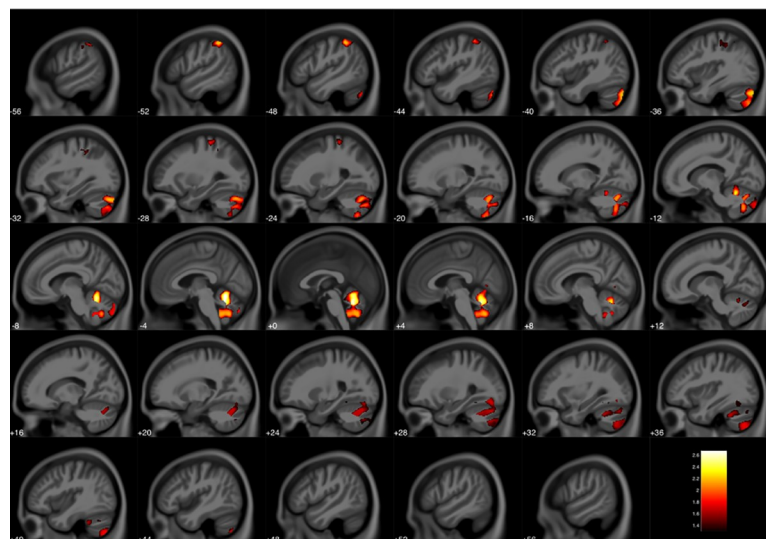


Fig 2. Reduced gray matter volume in the high ECAT group compared to the low ECAT group. Clusters were corrected for multiple comparisons using threshold free cluster enhancement with a familywise error rate of $p \leq 0.05$. Color bar represents $-\log(p)$ value.

<https://doi.org/10.1371/journal.pone.0228092.g002>

Table 4. Reduced gray matter volume in high ECAT exposure group compared to low ECAT exposure group with covariates.

Anatomical region	Cluster size (voxels)	Peak voxel MNI coordinates(X, Y, Z)	Voxel p-value
Left cerebellum	10731	-6-57-18	0.002
		-2-56-26	0.002
		-38-82-34	0.006
Right cerebellum	1258	40-70-54	0.016
		32-70-46	0.020
		30-84-44	0.028
	145	36-60-15	0.044
		30-50-14	0.047
Inferior parietal lobule	711	-51-46 51	0.006
		-56-33 44	0.039
		-52-33 52	0.046
Precentral gyrus	226	-34-39 48	0.034
		-34-30 50	0.036
		-28-44 51	0.037
	251	-27-33 63	0.016

Voxel and clusters corrected for multiple comparisons (FWE) at $P \leq 0.05$ using TFCE; ECAT = Elemental carbon attributable to traffic; FWE = Familywise error rate; MNI = Montreal neurological institute; TFCE = Threshold free cluster enhancement

<https://doi.org/10.1371/journal.pone.0228092.t004>

We also observed reduced gray matter volume in relation to increased TRAP exposure, primarily in the cerebellum, but also including the cerebellar vermis and the pre- and post-central gyri. This decrease was selective to gray matter and without a corresponding increase in white matter volume, which suggests the cerebellar changes are not due to a process of maturation, which would alter both gray and white matter. The cerebellum is primarily a modulatory brain region involved in the regulation of motor function, cognition, and emotion [52–56]. The cerebellum in particular grows rapidly in the first two years of life [57], with cerebellar injuries being related to cognitive developmental disorders [58] such as autism [59].

This combination of reduced cortical thickness primarily within the precentral gyrus and the reduced cerebellar volume implicates that the effects of TRAP impact two regions involved in motor function. Given these systems are early developing, they are more likely to be impacted by adverse insults such as environmental toxicants during critical developmental periods [60, 61]. Motor planning has been suggested to be related to cognitive performance and disorders such as anxiety [62–64].

Supporting evidence of prenatal exposure to TRAP

Early life exposure to TRAP have been previously described. Transplacental exposure to air pollutants with DNA adducts of polycyclic aromatic hydrocarbons (PAH) were measured in umbilical cord blood [65–67]. Placental expression of brain-derived neurotrophic factor (BDNF) and synapsin 1 (SYN1), two genes implicated in normal neurodevelopmental trajectories, decreased with increasing in utero exposure to $PM_{2.5}$ [68]. Direct or indirect maternal effects from air pollution, such as systemic low-grade inflammation, increased plasma viscosity, hormonal disruption or epigenetic changes, potentially impair placenta function and lead to neurological disruption by time of birth via mechanisms from decreased oxygen and nutrient transport [69].

Evidence of postnatal TRAP within the human central nervous system

Besides direct inhalation in postnatal life, other possible mechanisms for TRAP to cause detrimental central nervous system effects include translocation from the pulmonary,

gastrointestinal and circulatory systems [12, 70, 71]. Alterations in the blood brain barrier (BBB), disruption of endothelium, and microglial activation, accompanied by neuroinflammation, as well as the ability of TRAP to exert effects on the brain secondarily with cardiovascular dysfunction, all could potentially produce brain pathology [72–75]. Brain tissue from individuals, ages 2–45 years, living in highly polluted areas showed an increase in CD68, CD163, and HLA-DR antigens implicating infiltrating monocytes or resident microglia activation [75]. Upregulation of pro-inflammatory markers such as COX2 and IL1- β , and the CD14 markers for innate immune cells presented in the frontal cortex, vagus nerves and substantia nigra [75]. Increased A β 42 deposition, BBB disruption, endothelial cell activation [75], and brain lesions in the white matter of the prefrontal lobe were observed [75, 76]. Adolescent brains also featured significant amounts of lipofuscin in endothelial cortical capillaries [75]. Further studies demonstrated elevations hyper-phosphorylated tau and α -synuclein [77].

Evidence of TRAP exposure interfering with brain development in model systems

Early life TRAP exposures pose a substantial risk for interfering with normal brain development as constituent exposures may permanently harm the maturing cortex. Ejaz, Anwar [78] observed with histopathology and immunohistochemistry a positive dose-response relationship between PM exposure and severity of neuronal loss, predominately in the motor cortex and primary somatosensory cortex in rat models. Allen, Oberdorster [79] studied mice with an exposure models employing concentrated ambient ultrafine (UFP) particles with two exposure periods: postnatal day (PND) 4–7 and 10–13 (human 3rd trimester equivalent). This model employed the most reactive constituents measured in air pollution at levels representative of high traffic areas in major U.S. cities [79]. UFP exposures provoked inflammation and microglial activation, specifically, increased astrocytic activation in the amygdala [79]. Reductions in size of the corpus callosum were accompanied by hypomyelination, ventriculomegaly [79]. These models revealed elevated glutamate in both sexes, however, only males showed an altered ratio of glutamate and GABA with excitatory-inhibitory imbalance [79]. Finally, male mice in the models featured repetitive and impulsive behaviors [79]. The findings indicated the human 3rd trimester equivalent as potential susceptible to neurodevelopmental toxicity from UFP [79]. The results also supported the notion that exposure to UFP air pollution throughout periods of rapid neurodevelopment may increase the risk for developing ASD, and potentially other disorders such as ADHD, periventricular leukomalacia and schizophrenia [79].

Epidemiology of air pollution effects on mental health with imaging features

In children, epidemiologic evidence also supports a link between air pollution and ASD, ADHD, schizophrenia, developmental and cognitive delays [80–83]. Our group found evidence that each 0.25 mg/m³ increase in early life TRAP was associated with increases in depression and anxiety scores for the CCAAPS cohort [84]. In adults, there is similar evidence associating air pollution with measures of anxiety and depression [85–87]. Gestational and early childhood exposure to TRAP is associated with higher risk for schizophrenia, low birth weight and ASD [88]. Individuals with childhood onset schizophrenia demonstrated diffuse decreases in mean cortical thickness, with deficits localizing more anteriorly [89]. As reported by Newman, Ryan [80] using the Behavior Assessment System for Children, 2nd edition, exposure to the highest tertile of ECAT during the child's first year of life was significantly associated with hyperactivity T-scores in the "at-risk" range at 7 years of age for those participants

whose mothers had more than a high school education. ADHD has been associated with reductions in cortical thickness in prefrontal and precentral regions, and in the parietal lobe [90, 91]. The superior parietal lobule in particular appears to be heavily involved in attention [92–94] and is strongly associated with differences functional connectivity in ADHD [92, 95–98]. This may be due to a delay in the maturation [99] and functional development [97] of the cortex. Similarly, pediatric anxiety is related to differences in structural gray matter volumes [100], and Brunst, Ryan [101] found that myo-inositol may mediate anxiety levels in relation to TRAP exposure. Cerebellar abnormalities are consistently associated with numerous mental health disorders including anxiety, ADHD, ASD, and schizophrenia [55, 102–105]. Cerebellar volumes have been inversely correlated with depression and anxiety [106], and aberrant connectivity with other neural systems have been implicated as well [107, 108].

Cortical development, timing, thickness and volume

Cortical brain development in humans relies upon the division of progenitor cells within the ventricular zone of the germinal matrix [109]. The derived neurons and glia cells migrate outward toward the cortical plate and undergo a series of morphological changes where the cells differentiate and integrate into functional circuits. Cortical neurogenesis and migration are completed by the first week of postnatal life [110–112]. Subsequently, cortical development is largely dependent on dendritic growth, growth of the terminal axon arborization, myelination, and synaptogenesis [113–118]. Cerebral lamination in the developing fetus and at birth relies on the appearance and the resolution of the subplate, with subplate neurons that serve as a crucial regulator of cortical development [119]. Insults damaging one or more underlying cellular events during neurogenesis and migration can produce a variety of cortical changes [120]. Cortical thinning itself may indicate a loss of dendrites and dendritic spines and changes in myelination within specific brain systems [121, 122]. However, changes in cortical thickness and brain volume appropriately occur from in utero into adulthood with distinct regional timetables revealed noninvasively with fetal and postnatal neuroimaging [123]. During childhood, volumetric changes can occur from changes in neuronal size, neuropil, dendritic or axonal arborization or from the vasculature, synaptic proliferation and pruning, along with increasing myelination [124]. In the first two years of life, the human cerebral cortex undergoes marked expansion with the cortical surface area essentially doubling between birth and age 2 [118]. Lyall, Shi [125] found that cortical thickness by age 2 years reaches an estimated 97% of adult values, yet the corresponding cortical surface area is estimated at 69% adult values. Amlien, Fjell [126] explained cortical expansion of surface area and thickness across primate species as adhering to general allometric laws of scaling. They observed that cortical thickness showed a continuously negative trajectory for the range of 4 to 30 years of age across the entire cortex. In contrast, cortical surface area was positively related to age until about 12 years, with little subsequent differences. Gogtay, Giedd [127] conducted anatomical MRI examinations every two years between the ages of 4 and 21 years for 13 participants. Maturation of the cortex followed the evolutionary sequence in which the regions were created. Gray matter volumes peaked the earliest in primary sensorimotor areas and the latest in higher order association areas. The participants in the current study were imaged at age 12 years, which further supports that our findings are not related to changes occurring with the completion of typical cortical maturation associated with age, especially for sensorimotor regions.

Limitations

While our cohort is part of an ongoing, longitudinal evaluation of TRAP, our structural outcomes were ascertained based upon only one MRI examination and may be influenced by

interindividual variance or cohort effects. The high-low design targeting exposure during a given period (first year of life) and time of imaging at the same age (12 y) attempted to minimize the effects of changes in developmental maturation and unaccounted individual variances. However, if both groups are adversely impacted by TRAP, our approach may underestimate the effects due to our design. The regional specificity of the pre- and post-central gyri and the cerebellar gray matter findings with the absence of white matter volumetric findings suggests that these early developing structures incurred an insult altering their structural development. However, the structural evaluation of a single timepoint in an ongoing developmental process is a limitation. In the future, a longitudinal analysis with a second MRI evaluation is planned for this cohort as this is more sensitive to individual brain developmental patterns due to the exclusion of the influence of large interindividual variations. Also, we are unable to definitively exclude contributions from later childhood TRAP exposure with this analysis. However, given the key findings in structures that develop during the first and second trimester, it is plausible these structures have been impacted since the first year of life. It is also possible that our estimate of outdoor TRAP exposure at the participants' homes may not reflect daily personal exposures due to home characteristics that affect the outdoor-indoor penetration of pollutants and individual time-activity patterns of participants. However, estimating health effects associated with ambient pollutant concentrations offer the potential to guide regulatory limits and public health actions on a population-level. Also, inclusion criteria for the CCAAPS cohort required having at least one biological parent with atopy. Therefore, future studies should include children born to parents with and without allergic disease to confirm the generalizability of our results.

This study design along with the SPM12 (including CAT) software may limit the sensitivity of the analysis as there may be other regions with volume or cortical thickness changes beyond our ability to detect. We acknowledge this methodology is not well-suited for assessing volume differences in structures such as the hippocampus or amygdala. To minimize imaging processing effects, we analyzed the cortical thickness data using SPM12 and also with a rival software approach, known as Freesurfer [17], where a similar result was observed, but not shown. Future studies of cohorts evaluating TRAP should also include measures of sensory-motor function.

Conclusions

Our study found that children with higher levels of exposure to TRAP demonstrated regional reductions of cortical thickness and gray matter volume relative to children with lower levels. Reduced cortical thickness and volume loss in our study population are on the order of 3–4%. These findings are consistent with a process damaging the development of the sensorimotor cortex, frontal cortex, cerebellar vermis and cerebellar hemispheres as these structures form early in development and are vulnerable to injury.

Supporting information

S1 Fig. VBM and cortical thickness workflows in CAT12 toolbox.
(TIF)

Acknowledgments

The authors acknowledge the contribution of James Leach, MD, in reviewing the images for incidental clinical findings.

Author Contributions

Conceptualization: Kimberly Yolton, Grace LeMasters, Patrick Ryan.

Data curation: Rachel Severs, Christopher Wolfe, Zana Percy.

Formal analysis: Travis Beckwith, Mekibib Altaye, Thomas Maloney.

Funding acquisition: Kim Cecil, Kimberly Yolton, Grace LeMasters, Patrick Ryan.

Investigation: Kim Cecil, Rachel Severs, Christopher Wolfe, Zana Percy, Kimberly Yolton, Grace LeMasters, Patrick Ryan.

Methodology: Travis Beckwith, Kim Cecil, Mekibib Altaye, Thomas Maloney, Kimberly Yolton, Grace LeMasters, Patrick Ryan.

Project administration: Kim Cecil, Rachel Severs, Christopher Wolfe, Zana Percy, Patrick Ryan.

Resources: Kim Cecil, Kimberly Yolton, Patrick Ryan.

Supervision: Kim Cecil, Kimberly Yolton, Patrick Ryan.

Validation: Travis Beckwith, Kim Cecil, Mekibib Altaye, Patrick Ryan.

Visualization: Travis Beckwith.

Writing – original draft: Travis Beckwith, Kim Cecil, Kelly Brunst, Patrick Ryan.

Writing – review & editing: Travis Beckwith, Kim Cecil, Kelly Brunst, Patrick Ryan.

References

1. Block ML, Calderon-Garciduenas L. Air pollution: mechanisms of neuroinflammation and CNS disease. *Trends Neurosci.* 2009; 32(9):506–16. <https://doi.org/10.1016/j.tins.2009.05.009> PMID: 19716187
2. Chen H, Kwong JC, Copes R, Tu K, Villeneuve PJ, van Donkelaar A, et al. Living near major roads and the incidence of dementia, Parkinson's disease, and multiple sclerosis: a population-based cohort study. *Lancet.* 2017; 389(10070):718–26. [https://doi.org/10.1016/S0140-6736\(16\)32399-6](https://doi.org/10.1016/S0140-6736(16)32399-6) PMID: 28063597
3. Clifford A, Lang L, Chen R, Anstey KJ, Seaton A. Exposure to air pollution and cognitive functioning across the life course—A systematic literature review. *Environ Res.* 2016; 147:383–98. <https://doi.org/10.1016/j.envres.2016.01.018> PMID: 26945620
4. Costa LG, Cole TB, Coburn J, Chang YC, Dao K, Roque P. Neurotoxicants are in the air: convergence of human, animal, and in vitro studies on the effects of air pollution on the brain. *Biomed Res Int.* 2014; 2014:736385. <https://doi.org/10.1155/2014/736385> PMID: 24524086
5. Davis DA, Bortolato M, Godar SC, Sander TK, Iwata N, Pakbin P, et al. Prenatal exposure to urban air nanoparticles in mice causes altered neuronal differentiation and depression-like responses. *PLoS One.* 2013; 8(5):e64128. <https://doi.org/10.1371/journal.pone.0064128> PMID: 23734187
6. Flores-Pajot MC, Ofner M, Do MT, Lavigne E, Villeneuve PJ. Childhood autism spectrum disorders and exposure to nitrogen dioxide, and particulate matter air pollution: A review and meta-analysis. *Environ Res.* 2016; 151:763–76. <https://doi.org/10.1016/j.envres.2016.07.030> PMID: 27609410
7. Genc S, Zadeoglulari Z, Fuss SH, Genc K. The adverse effects of air pollution on the nervous system. *J Toxicol.* 2012; 2012:782462. <https://doi.org/10.1155/2012/782462> PMID: 22523490
8. Power MC, Adar SD, Yanosky JD, Weuve J. Exposure to air pollution as a potential contributor to cognitive function, cognitive decline, brain imaging, and dementia: A systematic review of epidemiologic research. *Neurotoxicology.* 2016; 56:235–53. <https://doi.org/10.1016/j.neuro.2016.06.004> PMID: 27328897
9. Suades-Gonzalez E, Gascon M, Guxens M, Sunyer J. Air pollution and neuropsychological development: a review of the latest evidence. *Endocrinology.* 2015; 156(10):3473–82. <https://doi.org/10.1210/en.2015-1403> PMID: 26241071

10. Costa LG, Cole TB, Coburn J, Chang YC, Dao K, Roque PJ. Neurotoxicity of traffic-related air pollution. *Neurotoxicology*. 2017; 59:133–9. <https://doi.org/10.1016/j.neuro.2015.11.008> PMID: 26610921
11. Oberdorster G, Sharp Z, Atudorei V, Elder A, Gelein R, Kreyling W, et al. Translocation of inhaled ultrafine particles to the brain. *Inhal Toxicol*. 2004; 16(6–7):437–45. <https://doi.org/10.1080/08958370490439597> PMID: 15204759
12. Oberdorster G, Sharp Z, Atudorei V, Elder A, Gelein R, Lunts A, et al. Extrapulmonary translocation of ultrafine carbon particles following whole-body inhalation exposure of rats. *J Toxicol Environ Health A*. 2002; 65(20):1531–43. <https://doi.org/10.1080/00984100290071658> PMID: 12396867
13. Peters A, Veronesi B, Calderon-Garciduenas L, Gehr P, Chen LC, Geiser M, et al. Translocation and potential neurological effects of fine and ultrafine particles a critical update. *Part Fibre Toxicol*. 2006; 3:13. <https://doi.org/10.1186/1743-8977-3-13> PMID: 16961926
14. Thompson PM, Hayashi KM, Sowell ER, Gogtay N, Giedd JN, Rapoport JL, et al. Mapping cortical change in Alzheimer's disease, brain development, and schizophrenia. *NeuroImage*. 2004; 23 Suppl 1:S2–18.
15. Vanasse TJ, Fox PM, Barron DS, Robertson M, Eickhoff SB, Lancaster JL, et al. BrainMap VBM: An environment for structural meta-analysis. *Hum Brain Mapp*. 2018; 39(8):3308–25. <https://doi.org/10.1002/hbm.24078> PMID: 29717540
16. Cecil KM, Brubaker CJ, Adler CM, Dietrich KN, Altaye M, Egelhoff JC, et al. Decreased brain volume in adults with childhood lead exposure. *PLoS Med*. 2008; 5(5):e112. <https://doi.org/10.1371/journal.pmed.0050112> PMID: 18507499
17. Fischl B, Dale AM. Measuring the thickness of the human cerebral cortex from magnetic resonance images. *Proc Natl Acad Sci U S A*. 2000; 97(20):11050–5. <https://doi.org/10.1073/pnas.200033797> PMID: 10984517
18. Ashburner J, Friston KJ. Voxel-based morphometry—the methods. *NeuroImage*. 2000; 11(6 Pt 1):805–21.
19. Jones SE, Buchbinder BR, Aharon I. Three-dimensional mapping of cortical thickness using Laplace's equation. *Hum Brain Mapp*. 2000; 11(1):12–32. [https://doi.org/10.1002/1097-0193\(200009\)11:1<12::aid-hbm20>3.0.co;2-k](https://doi.org/10.1002/1097-0193(200009)11:1<12::aid-hbm20>3.0.co;2-k) PMID: 10997850
20. Kabani N, Le Goualher G, MacDonald D, Evans AC. Measurement of cortical thickness using an automated 3-D algorithm: a validation study. *NeuroImage*. 2001; 13(2):375–80. <https://doi.org/10.1006/nimg.2000.0652> PMID: 11162277
21. Miller MI, Massie AB, Ratnanather JT, Botteron KN, Csernansky JG. Bayesian construction of geometrically based cortical thickness metrics. *NeuroImage*. 2000; 12(6):676–87. <https://doi.org/10.1006/nimg.2000.0666> PMID: 11112399
22. Panizzon MS, Fennema-Notestine C, Eyer LT, Jernigan TL, Prom-Wormley E, Neale M, et al. Distinct genetic influences on cortical surface area and cortical thickness. *Cereb Cortex*. 2009; 19(11):2728–35. <https://doi.org/10.1093/cercor/bhp026> PMID: 19299253
23. Ashburner J, Hutton C, Frackowiak R, Johnsrude I, Price C, Friston K. Identifying global anatomical differences: deformation-based morphometry. *Hum Brain Mapp*. 1998; 6(5–6):348–57. PMID: 9788071
24. Good CD, Johnsrude IS, Ashburner J, Henson RN, Friston KJ, Frackowiak RS. A voxel-based morphometric study of ageing in 465 normal adult human brains. *NeuroImage*. 2001; 14(1 Pt 1):21–36.
25. Hutton C, Draganski B, Ashburner J, Weiskopf N. A comparison between voxel-based cortical thickness and voxel-based morphometry in normal aging. *NeuroImage*. 2009; 48(2):371–80. <https://doi.org/10.1016/j.neuroimage.2009.06.043> PMID: 19559801
26. LeMasters GK, Wilson K, Levin L, Biagini J, Ryan P, Lockey JE, et al. High prevalence of aeroallergen sensitization among infants of atopic parents. *J Pediatr*. 2006; 149(4):505–11. <https://doi.org/10.1016/j.jpeds.2006.06.035> PMID: 17011322
27. Ryan PH, LeMasters G, Biagini J, Bernstein D, Grinshpun SA, Shukla R, et al. Is it traffic type, volume, or distance? Wheezing in infants living near truck and bus traffic. *J Allergy Clin Immunol*. 2005; 116(2):279–84. <https://doi.org/10.1016/j.jaci.2005.05.014> PMID: 16083780
28. Ryan PH, Lemasters GK, Levin L, Burkle J, Biswas P, Hu S, et al. A land-use regression model for estimating microenvironmental diesel exposure given multiple addresses from birth through childhood. *Sci Total Environ*. 2008; 404(1):139–47. <https://doi.org/10.1016/j.scitotenv.2008.05.051> PMID: 18625514
29. Ryan PH, Lemasters GK, Biswas P, Levin L, Hu S, Lindsey M, et al. A comparison of proximity and land use regression traffic exposure models and wheezing in infants. *Environ Health Perspect*. 2007; 115(2):278–84. <https://doi.org/10.1289/ehp.9480> PMID: 17384778

30. Hu S, McDonald R, Martuzevicius D, Biswas P, Grinshpun SA, Kelley A, et al. UNMIX modeling of ambient PM(2.5) near an interstate highway in Cincinnati, OH, USA. *Atmos Environ* (1994). 2006; 40 (S2):378–95.
31. Sahu M, Hu S, Ryan PH, Le Masters G, Grinshpun SA, Chow JC, et al. Chemical compositions and source identification of PM(2.5) aerosols for estimation of a diesel source surrogate. *Sci Total Environ*. 2011; 409(13):2642–51. <https://doi.org/10.1016/j.scitotenv.2011.03.032> PMID: 21496880
32. Gaser C, Dahnke R, editors. CAT—a computational anatomy toolbox for the analysis of structural MRI data. Poster presented at: 22nd Annual Meeting of the Organization for Human Brain Mapping; 2016 Jun 26–30; Geneva, Switzerland.
33. Beckwith TJ, Dietrich KN, Wright JP, Altaye M, Cecil KM. Reduced regional volumes associated with total psychopathy scores in an adult population with childhood lead exposure. *Neurotoxicology*. 2018; 67:1–26. <https://doi.org/10.1016/j.neuro.2018.04.004> PMID: 29634994
34. D’Agostino E, Maes F, Vandermeulen D, Suetens P. A unified framework for atlas based brain image segmentation and registration. In: International Workshop on Biomedical Image Registration 2006. p. 136–43.
35. Ashburner J. A fast diffeomorphic image registration algorithm. *NeuroImage*. 2007; 38(1):95–113. <https://doi.org/10.1016/j.neuroimage.2007.07.007> PMID: 17761438
36. Dahnke R, Yotter RA, Gaser C. Cortical thickness and central surface estimation. *NeuroImage*. 2013; 65:336–48. <https://doi.org/10.1016/j.neuroimage.2012.09.050> PMID: 23041529
37. Dahnke R, Ziegler G, Gaser C, editors. Local adaptive segmentation. Poster presented at: 18th Annual Meeting of the Organization for Human Brain Mapping; 2012 Jun 10–14; Beijing, China.
38. Yotter RA, Dahnke R, Thompson PM, Gaser C. Topological correction of brain surface meshes using spherical harmonics. *Hum Brain Mapp*. 2011; 32(7):1109–24. <https://doi.org/10.1002/hbm.21095> PMID: 20665722
39. Yotter RA, Thompson PM, Gaser C. Algorithms to improve the reparameterization of spherical mappings of brain surface meshes. *J Neuroimaging*. 2011; 21(2):e134–47. <https://doi.org/10.1111/j.1552-6569.2010.00484.x> PMID: 20412393
40. Yotter RA, Ziegler G, Thompson PM, Gaser C, editors. Diffeometric anatomical registration on the surface. Poster presented at: 17th Annual Meeting of the Organization for Human Brain Mapping; 2011 Jun 26–30; Québec City, Canada.
41. Gaser C. Threshold free cluster enhancement toolbox. <http://dbm.neuro.uni-jena.de/tfce/>.
42. Smith SM, Nichols TE. Threshold-free cluster enhancement: addressing problems of smoothing, threshold dependence and localisation in cluster inference. *NeuroImage*. 2009; 44(1):83–98. <https://doi.org/10.1016/j.neuroimage.2008.03.061> PMID: 18501637
43. Brokamp C, Beck AF, Goyal NK, Ryan P, Greenberg JM, Hall ES. Material community deprivation and hospital utilization during the first year of life: an urban population-based cohort study. *Ann Epidemiol*. 2019; 30:37–43. <https://doi.org/10.1016/j.annepidem.2018.11.008> PMID: 30563729
44. Guxens M, Lubczynska MJ, Muetzel RL, Dalmau-Bueno A, Jaddoe VVW, Hoek G, et al. Air pollution exposure during fetal life, brain morphology, and cognitive function in school-age children. *Biol Psychiatry*. 2018; 84(4):295–303. <https://doi.org/10.1016/j.biopsych.2018.01.016> PMID: 29530279
45. Bjuland KJ, Lohaugen GC, Martinussen M, Skranes J. Cortical thickness and cognition in very-low-birth-weight late teenagers. *Early Hum Dev*. 2013; 89(6):371–80. <https://doi.org/10.1016/j.earlhumdev.2012.12.003> PMID: 23273486
46. Haukvik UK, Rimol LM, Roddey JC, Hartberg CB, Lange EH, Vaskinn A, et al. Normal birth weight variation is related to cortical morphology across the psychosis spectrum. *Schizophr Bull*. 2014; 40 (2):410–9. <https://doi.org/10.1093/schbul/sbt005> PMID: 23419977
47. Joshi AA, Lepore N, Joshi SH, Lee AD, Barysheva M, Stein JL, et al. The contribution of genes to cortical thickness and volume. *Neuroreport*. 2011; 22(3):101–5. <https://doi.org/10.1097/WNR.0b013e3283424c84> PMID: 21233781
48. Ho KC, Roessmann U, Straumfjord JV, Monroe G. Analysis of brain weight. I. Adult brain weight in relation to sex, race, and age. *Arch Pathol Lab Med*. 1980; 104(12):635–9. PMID: 6893659
49. Rushton JP. Race, brain size, and intelligence: a reply to Cernovsky. *Psychol Rep*. 1990; 66(2):659–66. <https://doi.org/10.2466/pr0.1990.66.2.659> PMID: 2349356
50. Porro CA, Francescato MP, Cettolo V, Diamond ME, Baraldi P, Zuiani C, et al. Primary motor and sensory cortex activation during motor performance and motor imagery: a functional magnetic resonance imaging study. *J Neurosci*. 1996; 16(23):7688–98. <https://doi.org/10.1523/JNEUROSCI.16-23-07688.1996> PMID: 8922425

51. Corkin S, Milner B, Rasmussen T. Somatosensory thresholds—contrasting effects of postcentral-gyrus and posterior parietal-lobe excisions. *Arch Neurol*. 1970; 23(1):41–58. <https://doi.org/10.1001/archneur.1970.00480250045007> PMID: 4987142
52. Baumann O, Mattingley JB. Functional topography of primary emotion processing in the human cerebellum. *NeuroImage*. 2012; 61(4):805–11. <https://doi.org/10.1016/j.neuroimage.2012.03.044> PMID: 22465459
53. Holmes G. The Cerebellum of Man. *Brain*. 1939; 62(1):1–30.
54. Llinas R, Welsh JP. On the cerebellum and motor learning. *Curr Opin Neurobiol*. 1993; 3(6):958–65. [https://doi.org/10.1016/0959-4388\(93\)90168-x](https://doi.org/10.1016/0959-4388(93)90168-x) PMID: 8124080
55. Schmahmann JD. Disorders of the cerebellum: ataxia, dysmetria of thought, and the cerebellar cognitive affective syndrome. *J Neuropsychiatry Clin Neurosci*. 2004; 16(3):367–78. <https://doi.org/10.1176/jnp.16.3.367> PMID: 15377747
56. Schmahmann JD, Sherman JC. The cerebellar cognitive affective syndrome. *Brain*. 1998; 121 (Pt 4):561–79.
57. Knickmeyer RC, Gouttard S, Kang C, Evans D, Wilber K, Smith JK, et al. A structural MRI study of human brain development from birth to 2 years. *J Neurosci*. 2008; 28(47):12176–82. <https://doi.org/10.1523/JNEUROSCI.3479-08.2008> PMID: 19020011
58. Diamond A. Close interrelation of motor development and cognitive development and of the cerebellum and prefrontal cortex. *Child Dev*. 2000; 71(1):44–56. <https://doi.org/10.1111/1467-8624.00117> PMID: 10836557
59. Wang SS, Kloth AD, Badura A. The cerebellum, sensitive periods, and autism. *Neuron*. 2014; 83(3):518–32. <https://doi.org/10.1016/j.neuron.2014.07.016> PMID: 25102558
60. Rodier PM. Developing brain as a target of toxicity. *Environ Health Persp*. 1995; 103:73–6.
61. Weiss B. Vulnerability of children and the developing brain to neurotoxic hazards. *Environ Health Perspect*. 2000; 108 Suppl 3:375–81.
62. Mullen R, Hardy L, Tattersall A. The effects of anxiety on motor performance: A test of the conscious processing hypothesis. *J Sport Exercise Psy*. 2005; 27(2):212–25.
63. Eysenck MW, Derakshan N, Santos R, Calvo MG. Anxiety and cognitive performance: attentional control theory. *Emotion*. 2007; 7(2):336–53. <https://doi.org/10.1037/1528-3542.7.2.336> PMID: 17516812
64. Coombes SA, Higgins T, Gamble KM, Cauraugh JH, Janelle CM. Attentional control theory: anxiety, emotion, and motor planning. *J Anxiety Disord*. 2009; 23(8):1072–9. <https://doi.org/10.1016/j.janxdis.2009.07.009> PMID: 19674869
65. Edwards SC, Jedrychowski W, Butscher M, Camann D, Kieltyka A, Mroz E, et al. Prenatal exposure to airborne polycyclic aromatic hydrocarbons and children's intelligence at 5 years of age in a prospective cohort study in Poland. *Environ Health Perspect*. 2010; 118(9):1326–31. <https://doi.org/10.1289/ehp.0901070> PMID: 20406721
66. Perera FP, Rauh V, Whyatt RM, Tsai WY, Tang D, Diaz D, et al. Effect of prenatal exposure to airborne polycyclic aromatic hydrocarbons on neurodevelopment in the first 3 years of life among inner-city children. *Environ Health Perspect*. 2006; 114(8):1287–92. <https://doi.org/10.1289/ehp.9084> PMID: 16882541
67. Tang D, Li TY, Liu JJ, Zhou ZJ, Yuan T, Chen YH, et al. Effects of prenatal exposure to coal-burning pollutants on children's development in China. *Environ Health Perspect*. 2008; 116(5):674–9. <https://doi.org/10.1289/ehp.10471> PMID: 18470301
68. Saenen ND, Plusquin M, Bijlens E, Janssen BG, Gyselaers W, Cox B, et al. In utero fine particle air pollution and placental expression of genes in the brain-derived neurotrophic factor signaling pathway: an ENVIRONAGE birth cohort study. *Environ Health Perspect*. 2015; 123(8):834–40. <https://doi.org/10.1289/ehp.1408549> PMID: 25816123
69. Sunyer J, Davdand P. Prenatal brain development as a target for urban air pollution. *Basic Clin Pharmacol Toxicol*. 2019.
70. Cassee FR, Heroux ME, Gerlofs-Nijland ME, Kelly FJ. Particulate matter beyond mass: recent health evidence on the role of fractions, chemical constituents and sources of emission. *Inhal Toxicol*. 2013; 25(14):802–12. <https://doi.org/10.3109/08958378.2013.850127> PMID: 24304307
71. Seaton A, MacNee W, Donaldson K, Godden D. Particulate air pollution and acute health effects. *Lancet*. 1995; 345(8943):176–8. [https://doi.org/10.1016/s0140-6736\(95\)90173-6](https://doi.org/10.1016/s0140-6736(95)90173-6) PMID: 7741860
72. Calderon-Garciduenas L, Azzarelli B, Acuna H, Garcia R, Gambling TM, Osnaya N, et al. Air pollution and brain damage. *Toxicol Pathol*. 2002; 30(3):373–89. <https://doi.org/10.1080/01926230252929954> PMID: 12051555

73. Calderon-Garciduenas L, Maronpot RR, Torres-Jardon R, Henriquez-Roldan C, Schoonhoven R, Acuna-Ayala H, et al. DNA damage in nasal and brain tissues of canines exposed to air pollutants is associated with evidence of chronic brain inflammation and neurodegeneration. *Toxicol Pathol.* 2003; 31(5):524–38. <https://doi.org/10.1080/01926230390226645> PMID: 14692621
74. Calderon-Garciduenas L, Reed W, Maronpot RR, Henriquez-Roldan C, Delgado-Chavez R, Calderon-Garciduenas A, et al. Brain inflammation and Alzheimer's-like pathology in individuals exposed to severe air pollution. *Toxicologic Pathology.* 2004; 32(6):650–8. <https://doi.org/10.1080/01926230490520232> PMID: 15513908
75. Calderon-Garciduenas L, Solt AC, Henriquez-Roldan C, Torres-Jardon R, Nuse B, Herritt L, et al. Long-term air pollution exposure is associated with neuroinflammation, an altered innate immune response, disruption of the blood-brain barrier, ultrafine particulate deposition, and accumulation of amyloid beta-42 and alpha-synuclein in children and young adults. *Toxicol Pathol.* 2008; 36(2):289–310. <https://doi.org/10.1177/0192623307313011> PMID: 18349428
76. Calderon-Garciduenas L, Mora-Tiscareno A, Ontiveros E, Gomez-Garza G, Barragan-Mejia G, Broadway J, et al. Air pollution, cognitive deficits and brain abnormalities: a pilot study with children and dogs. *Brain Cogn.* 2008; 68(2):117–27. <https://doi.org/10.1016/j.bandc.2008.04.008> PMID: 18550243
77. Calderon-Garciduenas L, Kavanaugh M, Block M, D'Angiulli A, Delgado-Chavez R, Torres-Jardon R, et al. Neuroinflammation, hyperphosphorylated tau, diffuse amyloid plaques, and down-regulation of the cellular prion protein in air pollution exposed children and young adults. *J Alzheimers Dis.* 2012; 28(1):93–107. <https://doi.org/10.3233/JAD-2011-110722> PMID: 21955814
78. Ejaz S, Anwar K, Ashraf M. MRI and neuropathological validations of the involvement of air pollutants in cortical selective neuronal loss. *Environ Sci Pollut Res Int.* 2014; 21(5):3351–62. <https://doi.org/10.1007/s11356-013-2294-5> PMID: 24234816
79. Allen JL, Oberdorster G, Morris-Schaffer K, Wong C, Klocke C, Sobolewski M, et al. Developmental neurotoxicity of inhaled ambient ultrafine particle air pollution: Parallels with neuropathological and behavioral features of autism and other neurodevelopmental disorders. *Neurotoxicology.* 2017; 59:140–54. <https://doi.org/10.1016/j.neuro.2015.12.014> PMID: 26721665
80. Newman NC, Ryan P, LeMasters G, Levin L, Bernstein D, Hershey GKK, et al. Traffic-related air pollution exposure in the first year of life and behavioral scores at 7 years of age. *Environ Health Perspect.* 2013; 121(6):731–6. <https://doi.org/10.1289/ehp.1205555> PMID: 23694812
81. Pedersen CB, Raaschou-Nielsen O, Hertel O, Mortensen PB. Air pollution from traffic and schizophrenia risk. *Schizophr Res.* 2004; 66(1):83–5. [https://doi.org/10.1016/s0920-9964\(03\)00062-8](https://doi.org/10.1016/s0920-9964(03)00062-8) PMID: 14693358
82. Sunyer J, Esnaola M, Alvarez-Pedrerol M, Forns J, Rivas I, Lopez-Vicente M, et al. Association between traffic-related air pollution in schools and cognitive development in primary school children: a prospective cohort study. *Plos Med.* 2015; 12(3):e1001792. <https://doi.org/10.1371/journal.pmed.1001792> PMID: 25734425
83. Volk HE, Lurmann F, Penfold B, Hertz-Picciotto I, McConnell R. Traffic-related air pollution, particulate matter, and autism. *JAMA Psychiatry.* 2013; 70(1):71–7. <https://doi.org/10.1001/jamapsychiatry.2013.266> PMID: 23404082
84. Yolton K, Khoury JC, Burkle J, LeMasters G, Cecil K, Ryan P. Lifetime exposure to traffic-related air pollution and symptoms of depression and anxiety at age 12 years. *Environ Res.* 2019; 173:199–206. <https://doi.org/10.1016/j.envres.2019.03.005> PMID: 30925441
85. Pun VC, Manjourides J, Suh H. Association of ambient air pollution with depressive and anxiety symptoms in older adults: results from the NSHAP study. *Environ Health Perspect.* 2017; 125(3):342–8. <https://doi.org/10.1289/EHP494> PMID: 27517877
86. Vert C, Sanchez-Benavides G, Martinez D, Gotsens X, Gramunt N, Cirach M, et al. Effect of long-term exposure to air pollution on anxiety and depression in adults: A cross-sectional study. *Int J Hyg Environ Health.* 2017; 220(6):1074–80. <https://doi.org/10.1016/j.ijheh.2017.06.009> PMID: 28705430
87. Power MC, Kioumourtoglou MA, Hart JE, Okereke OI, Laden F, Weisskopf MG. The relation between past exposure to fine particulate air pollution and prevalent anxiety: observational cohort study. *BMJ.* 2015; 350:h1111. <https://doi.org/10.1136/bmj.h1111> PMID: 25810495
88. Woodward N, Finch CE, Morgan TE. Traffic-related air pollution and brain development. *AIMS Environ Sci.* 2015; 2(2):353–73. <https://doi.org/10.3934/environsci.2015.2.353> PMID: 27099868
89. Greenstein D, Lerch J, Shaw P, Clasen L, Giedd J, Gochman P, et al. Childhood onset schizophrenia: cortical brain abnormalities as young adults. *J Child Psychol Psychiatry.* 2006; 47(10):1003–12. <https://doi.org/10.1111/j.1469-7610.2006.01658.x> PMID: 17073979
90. Almeida Montes LG, Prado Alcantara H, Martinez Garcia RB, De La Torre LB, Avila Acosta D, Duarte MG. Brain cortical thickness in ADHD: age, sex, and clinical correlations. *J Atten Disord.* 2013; 17(8):641–54. <https://doi.org/10.1177/1087054711434351> PMID: 22392552

91. Shaw P, Lerch J, Greenstein D, Sharp W, Clasen L, Evans A, et al. Longitudinal mapping of cortical thickness and clinical outcome in children and adolescents with attention-deficit/hyperactivity disorder. *Arch Gen Psychiatry*. 2006; 63(5):540–9. <https://doi.org/10.1001/archpsyc.63.5.540> PMID: 16651511
92. Park BY, Park H. Connectivity differences between adult male and female patients with attention deficit hyperactivity disorder according to resting-state functional MRI. *Neural Regen Res*. 2016; 11(1):119–25. <https://doi.org/10.4103/1673-5374.175056> PMID: 26981099
93. Molenberghs P, Mesulam MM, Peeters R, Vandenberghe RR. Remapping attentional priorities: differential contribution of superior parietal lobule and intraparietal sulcus. *Cereb Cortex*. 2007; 17(11):2703–12. <https://doi.org/10.1093/cercor/bhl179> PMID: 17264251
94. Kamali A, Sair HI, Radmanesh A, Hasan KM. Decoding the superior parietal lobule connections of the superior longitudinal fasciculus/arcuate fasciculus in the human brain. *Neuroscience*. 2014; 277:577–83. <https://doi.org/10.1016/j.neuroscience.2014.07.035> PMID: 25086308
95. Wolf RC, Plichta MM, Sambataro F, Fallgatter AJ, Jacob C, Lesch KP, et al. Regional brain activation changes and abnormal functional connectivity of the ventrolateral prefrontal cortex during working memory processing in adults with attention-deficit/hyperactivity disorder. *Hum Brain Mapp*. 2009; 30(7):2252–66. <https://doi.org/10.1002/hbm.20665> PMID: 19107748
96. Shang CY, Sheng C, Yang LK, Chou TL, Gau SS. Differential brain activations in adult attention-deficit/hyperactivity disorder subtypes: a counting Stroop functional MRI study. *Brain Imaging Behav*. 2018; 12(3):882–90. <https://doi.org/10.1007/s11682-017-9749-0> PMID: 28699075
97. Marcos-Vidal L, Martinez-Garcia M, Pretus C, Garcia-Garcia D, Martinez K, Janssen J, et al. Local functional connectivity suggests functional immaturity in children with attention-deficit/hyperactivity disorder. *Hum Brain Mapp*. 2018; 39(6):2442–54. <https://doi.org/10.1002/hbm.24013> PMID: 29473262
98. Poissant H, Rapin L, Mendrek A. Intergenerational transmission of fronto-parietal dysfunction during forethought in attention deficit/hyperactivity disorder: A pilot study. *Psychiat Res-Neuroim*. 2014; 224(3):242–5.
99. Shaw P, Eckstrand K, Sharp W, Blumenthal J, Lerch JP, Greenstein D, et al. Attention-deficit/hyperactivity disorder is characterized by a delay in cortical maturation. *Proc Natl Acad Sci U S A*. 2007; 104(49):19649–54. <https://doi.org/10.1073/pnas.0707741104> PMID: 18024590
100. Strawn JR, Hamm L, Fitzgerald DA, Fitzgerald KD, Monk CS, Phan KL. Neurostructural abnormalities in pediatric anxiety disorders. *J Anxiety Disord*. 2015; 32:81–8. <https://doi.org/10.1016/j.janxdis.2015.03.004> PMID: 25890287
101. Brunst KJ, Ryan PH, Altaye M, Yolton K, Maloney T, Beckwith T, et al. Myo-inositol mediates the effects of traffic-related air pollution on generalized anxiety symptoms at age 12years. *Environ Res*. 2019; 175:71–8. <https://doi.org/10.1016/j.envres.2019.05.009> PMID: 31103795
102. Stanfield AC, McIntosh AM, Spencer MD, Philip R, Gaur S, Lawrie SM. Towards a neuroanatomy of autism: a systematic review and meta-analysis of structural magnetic resonance imaging studies. *Eur Psychiatry*. 2008; 23(4):289–99. <https://doi.org/10.1016/j.eurpsy.2007.05.006> PMID: 17765485
103. Valera EM, Faraone SV, Murray KE, Seidman LJ. Meta-analysis of structural imaging findings in attention-deficit/hyperactivity disorder. *Biol Psychiatry*. 2007; 61(12):1361–9. <https://doi.org/10.1016/j.biopsych.2006.06.011> PMID: 16950217
104. Schmahmann JD, Weilburg JB, Sherman JC. The neuropsychiatry of the cerebellum—insights from the clinic. *Cerebellum*. 2007; 6(3):254–67. <https://doi.org/10.1080/14734220701490995> PMID: 17786822
105. Schutter DJ, van Honk J. The cerebellum on the rise in human emotion. *Cerebellum*. 2005; 4(4):290–4. <https://doi.org/10.1080/14734220500348584> PMID: 16321885
106. Schutter DJ, Koolschijn PC, Peper JS, Crone EA. The cerebellum link to neuroticism: a volumetric MRI association study in healthy volunteers. *PLoS One*. 2012; 7(5):e37252. <https://doi.org/10.1371/journal.pone.0037252> PMID: 22615955
107. Moreno-Rius J. The cerebellum in fear and anxiety-related disorders. *Prog Neuropsychopharmacol Biol Psychiatry*. 2018; 85:23–32. <https://doi.org/10.1016/j.pnpbp.2018.04.002> PMID: 29627508
108. Caulfield MD, Servatius RJ. Focusing on the possible role of the cerebellum in anxiety disorders. *New Insights into Anxiety Disorders*: IntechOpen; 2013. p. 41–70.
109. Rakic P. Specification of cerebral cortical areas. *Science*. 1988; 241(4862):170–6. <https://doi.org/10.1126/science.3291116> PMID: 3291116
110. Clowry G, Molnar Z, Rakic P. Renewed focus on the developing human neocortex. *J Anat*. 2010; 217(4):276–88. <https://doi.org/10.1111/j.1469-7580.2010.01281.x> PMID: 20979582
111. Rakic P. Evolution of the neocortex: a perspective from developmental biology. *Nat Rev Neurosci*. 2009; 10(10):724–35. <https://doi.org/10.1038/nrn2719> PMID: 19763105

112. Hill J, Inder T, Neil J, Dierker D, Harwell J, Van Essen D. Similar patterns of cortical expansion during human development and evolution. *Proc Natl Acad Sci U S A*. 2010; 107(29):13135–40. <https://doi.org/10.1073/pnas.1001229107> PMID: 20624964
113. Mrzljak L, Uylings HB, Van Eden CG, Judas M. Neuronal development in human prefrontal cortex in prenatal and postnatal stages. *Prog Brain Res*. 1990; 85:185–222. [https://doi.org/10.1016/s0079-6123\(08\)62681-3](https://doi.org/10.1016/s0079-6123(08)62681-3) PMID: 2094894
114. Koenderink MJ, Uylings HB. Postnatal maturation of layer V pyramidal neurons in the human prefrontal cortex. A quantitative Golgi analysis. *Brain Res*. 1995; 678(1–2):233–43. [https://doi.org/10.1016/0006-8993\(95\)00206-6](https://doi.org/10.1016/0006-8993(95)00206-6) PMID: 7542541
115. Koenderink MJ, Uylings HB, Mrzljak L. Postnatal maturation of the layer III pyramidal neurons in the human prefrontal cortex: a quantitative Golgi analysis. *Brain Res*. 1994; 653(1–2):173–82. [https://doi.org/10.1016/0006-8993\(94\)90387-5](https://doi.org/10.1016/0006-8993(94)90387-5) PMID: 7982051
116. Rakic P, Bourgeois JP, Goldman-Rakic PS. Synaptic development of the cerebral cortex: implications for learning, memory, and mental illness. *Prog Brain Res*. 1994; 102:227–43. [https://doi.org/10.1016/S0079-6123\(08\)60543-9](https://doi.org/10.1016/S0079-6123(08)60543-9) PMID: 7800815
117. Petanjek Z, Judas M, Simic G, Rasin MR, Uylings HB, Rakic P, et al. Extraordinary neoteny of synaptic spines in the human prefrontal cortex. *Proc Natl Acad Sci U S A*. 2011; 108(32):13281–6. <https://doi.org/10.1073/pnas.1105108108> PMID: 21788513
118. Li G, Nie J, Wang L, Shi F, Lin W, Gilmore JH, et al. Mapping region-specific longitudinal cortical surface expansion from birth to 2 years of age. *Cereb Cortex*. 2013; 23(11):2724–33. <https://doi.org/10.1093/cercor/bhs265> PMID: 22923087
119. Kanold PO. Subplate neurons: crucial regulators of cortical development and plasticity. *Front Neuroanat*. 2009; 3:16. <https://doi.org/10.3389/neuro.05.016.2009> PMID: 19738926
120. Gleeson JG, Walsh CA. Neuronal migration disorders: from genetic diseases to developmental mechanisms. *Trends Neurosci*. 2000; 23(8):352–9. [https://doi.org/10.1016/s0166-2236\(00\)01607-6](https://doi.org/10.1016/s0166-2236(00)01607-6) PMID: 10906798
121. Benes FM. Why does psychosis develop during adolescence and early adulthood? *Current Opinion in Psychiatry*. 2003; 16(3):317–9.
122. Harrison PJ. The neuropathology of schizophrenia. A critical review of the data and their interpretation. *Brain*. 1999; 122 (Pt 4):593–624.
123. Walhovd KB, Fjell AM, Giedd J, Dale AM, Brown TT. Through thick and thin: a need to reconcile contradictory results on trajectories in human cortical development. *Cereb Cortex*. 2016; 27(2):bhv301.
124. Giedd JN, Blumenthal J, Jeffries NO, Castellanos FX, Liu H, Zijdenbos A, et al. Brain development during childhood and adolescence: a longitudinal MRI study. *Nat Neurosci*. 1999; 2(10):861–3. <https://doi.org/10.1038/13158> PMID: 10491603
125. Lyall AE, Shi F, Geng X, Woolson S, Li G, Wang L, et al. Dynamic development of regional cortical thickness and surface area in early childhood. *Cereb Cortex*. 2015; 25(8):2204–12. <https://doi.org/10.1093/cercor/bhu027> PMID: 24591525
126. Amlien IK, Fjell AM, Tamnes CK, Grydeland H, Krogsrud SK, Chaplin TA, et al. Organizing principles of human cortical development—thickness and area from 4 to 30 years: insights from comparative primate neuroanatomy. *Cereb Cortex*. 2016; 26(1):257–67. <https://doi.org/10.1093/cercor/bhu214> PMID: 25246511
127. Gogtay N, Giedd JN, Lusk L, Hayashi KM, Greenstein D, Vaituzis AC, et al. Dynamic mapping of human cortical development during childhood through early adulthood. *Proc Natl Acad Sci U S A*. 2004; 101(21):8174–9. <https://doi.org/10.1073/pnas.0402680101> PMID: 15148381